

RESEARCH

Open Access



Lactate links exercise to synaptic protection and cognitive enhancement in Alzheimer's disease models

Hao Han¹, Yi Wu², Ru Mi¹, Cijia Zhang¹, Fengying Guan¹, Xiaoyan Lu³, Guangwei Zhang⁴, Zhaojie Meng⁵, Li Chen¹ and Ming Zhang^{1*}

Abstract

Background Physical exercise is known to promote cognitive resilience in aging and Alzheimer's disease (AD), but the underlying mechanisms remain incompletely understood. Lactate, a metabolic byproduct elevated during exercise, has recently emerged as a potential neuromodulator of brain function.

Methods Three AD-like mouse models (SAMP8, A β 1-42 injection, and 5xFAD) were used to evaluate the effects of treadmill exercise on cognitive function and synaptic plasticity. Serum lactate levels were assessed, and sodium L-lactate (NaLA) was administered to determine its neuroprotective effects. Transcriptomic analysis was performed on hippocampal tissue to explore lactate-regulated pathways. Lactate transport was pharmacologically inhibited using 4-CIN for mechanistic validation.

Results Treadmill exercise significantly improved cognitive performance and increased synapse-associated protein expression in AD models. Exercise elevated serum lactate levels, and exogenous NaLA administration recapitulated the cognitive and synaptic benefits of exercise. Transcriptomic profiling revealed enrichment of genes involved in axon guidance and synaptic organization, including upregulation of multiple Eph receptor family genes. α -cyano-4-hydroxycinnamic acid (4-CIN) administration abolished the exercise-induced neuroprotective effects, confirming the essential role of lactate transport in mediating these benefits.

Conclusions This study identifies lactate as a critical mediator linking exercise to enhanced synaptic function and cognitive improvement in AD-like models, providing mechanistic insights and highlighting lactate metabolism as a potential therapeutic target for AD.

Keywords Alzheimer's disease, Exercise, Lactate, Synaptic plasticity, Cognitive function, Axon guidance

*Correspondence:

Ming Zhang
zhangming99@jlu.edu.cn

¹ Department of Pharmacology, College of Basic Medical Sciences, Key Laboratory of Pathobiology, Ministry of Education, Jilin University, 126 Xin Min Street, Changchun, Jilin 130021, China

² Jilin Provincial Institute of Pharmaceutical Research, Changchun 130061, China

³ The Second Hospital of Jilin University, Changchun 130041, China

⁴ The First Hospital of Jilin University, Changchun 130031, China

⁵ State Key Laboratory of Respiratory Disease, National Clinical Research Center for Respiratory Disease, National Center for Respiratory Medicine, Guangzhou Institute of Respiratory Health, The First Affiliated Hospital of Guangzhou Medical University, Guangzhou 510000, China



Background

AD is a progressive neurodegenerative disorder characterized by memory loss, cognitive decline, and behavioral dysfunction [1]. The accumulation of amyloid- β (A β) peptides and the formation of extracellular plaques are considered early and central events in AD pathogenesis [2]. Soluble A β oligomers are highly neurotoxic and have been shown to disrupt synaptic signaling, leading to dendritic spine loss, synaptic degeneration, and ultimately impaired learning and memory [3, 4].

Currently, treatment options for AD remain limited, costly, and largely ineffective, with no curative drugs available to halt disease progression [5]. This has prompted increasing attention toward modifiable risk factors and early preventive strategies. Among these, non-pharmacological, lifestyle-based interventions are gaining recognition as promising approaches to delay or mitigate AD-related decline [6, 7]. Accumulating evidence suggests that physical exercise enhances cognitive performance and attenuates neurodegenerative processes associated with AD [8–10]. Clinical studies in older adults have shown that aerobic exercise increases hippocampal volume and improves spatial memory function [11]. Parallel findings from animal models demonstrate that exercise alleviates neuronal degeneration, reverses synaptic loss, and restores presynaptic vesicle density in AD brains [12–14]. These effects are thought to be mediated, at least in part, by the upregulation of genes involved in learning, memory, synaptic plasticity, and neuronal survival [15]. However, as a systemic intervention, exercise induces complex molecular adaptations across multiple tissues, and the specific mediators linking peripheral metabolic changes to central synaptic remodeling remain insufficiently understood.

Recent studies have confirmed the potential link between exercise-induced metabolic factors (such as β -Hydroxybutyrate and lactate) and muscle-derived myokines (such as Gpld1 and irisin) with improvements in brain function [16–20]. These molecules are released into circulation during exercise and can cross the blood-brain barrier (BBB), where they influence neurogenesis, neuronal survival, and synaptic plasticity [20, 21]. Among these candidates, lactate has attracted increasing attention due to its dual role as both an energy substrate and a signaling molecule. During exercise, enhanced glycolytic activity in skeletal muscle leads to a marked increase in circulating lactate levels, which can subsequently enter the brain via monocarboxylate transporters (MCTs) [22, 23]. High levels of MCT2 expression have been detected in neurons, where it facilitates the uptake of lactate [24, 25]. Emerging evidence suggests that lactate not only serves as an energy source to support the metabolic demands of neurons, but also promotes learning and

memory processes by modulating brain neuroplasticity [26, 27]. L-lactate has been shown to induce the expression of immediate early genes such as Arc, Egr1, Zif268, and c-Fos, which play essential roles in synaptic plasticity and long-term potentiation (LTP) [28]. In addition, lactate can enhance brain-derived neurotrophic factor (BDNF) expression through activation of the SIRT1–PGC1 α –FNDC5 pathway, thereby supporting neuronal survival and synaptogenesis [26, 29]. Together, these findings support the growing view that lactate acts not only as a metabolic fuel but also as a molecular effector that bridges peripheral exercise-induced metabolic changes with central nervous system function. However, the mechanisms by which it contributes to exercise-induced cognitive benefits in AD remain to be fully elucidated.

In this study, we investigated whether lactate mediates the cognitive improvements induced by exercise using three complementary AD-like mouse models: SAMP8, hippocampal A β 1–42 injection, and 5xFAD transgenic mice. We further examined whether exogenous lactate administration could replicate the beneficial effects of exercise, and whether inhibition of lactate transport would abolish them. Transcriptomic profiling was also conducted to identify lactate-responsive molecular pathways. These findings may help clarify the role of lactate in exercise-induced cognitive improvement and provide insights into its potential contribution to Alzheimer's disease pathology.

Methods

Animals

SAMP8 and SAMR1 mice (11 weeks old) were purchased from Beijing Weixuan Technology Co., Ltd. (Beijing, China), and acclimated for 1 week before experimental interventions.

For the A β 1–42 oligomer-induced AD model, A β 1–42 peptides (Abcam, UK) were prepared into oligomeric forms as described previously [30]. The peptide films were dissolved in DMSO (5 mM), diluted with sterile PBS to 100 μ M, and incubated at 4 °C for 24 h. C57BL/6 J mice (Yisi Experimental Animal Technology Co., Ltd., Changchun, China) were anesthetized with 1% pentobarbital sodium and placed in a stereotaxic apparatus. A β 1–42 oligomers (5 μ L, 100 μ M) were bilaterally injected into the hippocampus (AP: –2.0 mm, ML: \pm 1.5 mm, DV: –2.0 mm) at a rate of 0.5 μ L/min. The needle was retained for 5 min to prevent reflux. Sham mice received an equal volume of PBS. Mice were allowed 1 week of recovery before subsequent interventions.

5xFAD transgenic mice (12 weeks old) were purchased from Cavens Laboratory Animal Co., Ltd. (Changzhou, China), and age-matched wild-type littermates were used

as controls. All mice were acclimated for 1 week prior to experimentation.

For all experiments, only male mice were used to minimize sex-related variability. Each experimental group included 10–15 mice, depending on the specific behavioral, molecular, or histological analyses performed. The mice were housed in a room with suitable temperature and maintained on a 12 h day/night cycle. All animal procedures were approved by the Ethics Committee of Jilin University [SYXK(JI)2024–0023] and conducted in accordance with the ARRIVE guidelines.

Exercise training protocol

Treadmill exercise intervention was conducted using a motorized rodent treadmill (Taimeng, Chengdu, China). Mice first underwent a 3-day adaptation period with gradually increasing speeds (5 m/min, 10 m/min, and 15 m/min, respectively). Formal training commenced on day 4, consisting of running at a 5° incline, 15 m/min for 40 min per session, 5 days per week for 8 consecutive weeks. The running speed was increased by 1 m/min each week to progressively enhance exercise intensity. Throughout the intervention, mice were closely monitored for behavioral status, and body weight was recorded regularly.

For 5xFAD mice in the 4-CIN group, a physiological saline solution of 4-CIN (200 mg/kg, Selleck Chemicals, Houston, USA) was administered intraperitoneally 1 h prior to each exercise session throughout the intervention period.

NaLA administration

In the Aβ1–42 injection model, NaLA (Sigma-Aldrich, St. Louis, USA) was administered via intraperitoneal injection at a dose of 2 g/kg, 5 days per week for 8 consecutive weeks. Throughout the intervention, mice were closely monitored for general health status and behavioral activity, and body weight was recorded regularly.

Lactate measurement

Blood lactate levels were measured using a portable lactate meter (VivaChek, Hangzhou, China). Tail vein blood was collected 15 min after treadmill exercise or intraperitoneal NaLA administration.

Y-maze test

After the final intervention, animals were transferred to the behavioral testing room and maintained under standard housing conditions for 24 h to acclimate to the new environment. Behavioral testing was initiated 24 h later.

The Y-maze apparatus consisted of three arms (30 cm long, 6 cm wide, and 15 cm high) arranged at 120° angles, designated as the start arm, novel arm, and other arm.

During the training phase, the novel arm was blocked, and each mouse was placed at the end of the start arm and allowed to freely explore the other two arms for 8 min. After a 4-h retention interval, the novel arm was opened, and the mouse was reintroduced into the start arm for the test phase. Behavioral activity was recorded and analyzed using Smart 3.0 software (PanLab, Barcelona, Spain).

Morris water maze test

The spatial learning and memory ability of mice was assessed using the Morris water maze (MWM), following our previously established protocol [31]. The test was conducted in a circular pool (diameter: 150 cm; water depth: 16 cm; water temperature: 26 °C). To obscure the submerged platform, the water was made opaque by adding non-toxic white paint. The pool was virtually divided into four quadrants, with a hidden platform placed in one of them.

The test consisted of 5 days of training trials and a probe trial on the sixth day. During each training session, mice were released from various starting positions and given 60 s to locate the hidden platform. If a mouse failed to find the platform within the allotted time, it was gently guided to the platform and allowed to remain there for 15 s to aid spatial learning. On the sixth day, the platform was removed, and mice were allowed to swim freely for 60 s. The percentage of time spent in the target quadrant and swimming trajectories were recorded to assess memory retention performance. Animal behavior was recorded and analyzed using Smart 3.0 software (PanLab, Barcelona, Spain).

Novel object recognition test

The novel object recognition (NOR) test was used to evaluate recognition memory based on the innate tendency of rodents to explore novel stimuli. The apparatus consisted of a square open-field arena (40 cm × 40 cm × 40 cm). On the day prior to the formal test, each mouse was individually placed in the empty arena and allowed to freely explore for 10 min to habituate to the environment. The experiment consisted of two phases: familiarization and test. During the familiarization phase, two identical objects (Object A and Object B) were placed in opposite corners of the arena, and each mouse was allowed to explore freely for 10 min. After a 4-h interval, one of the familiar objects was replaced with a novel object, and the mice were returned to the arena for a 5-min test session. All behaviors were recorded and analyzed using Smart 3.0 software (PanLab, Barcelona, Spain). Exploration was defined as the mouse directing its nose toward or sniffing the object within a distance of ≤ 2 cm.

The recognition index was calculated as:

$$\text{Recognition index (\%)} = [\text{Time (novel object)} / (\text{Time (novel)} + \text{Time (familiar)})] \times 100\%.$$

Animal euthanasia and tissue collection

Animals were euthanized 24 h after the final behavioral test to ensure the stabilization of physiological responses. Euthanasia was conducted via intraperitoneal injection of pentobarbital sodium (50 mg/kg), followed by transcardial perfusion with ice-cold saline. Brain tissues were subsequently either fixed in 4% paraformaldehyde or snap-frozen in liquid nitrogen, depending on the requirements of downstream analyses.

HE staining and Nissl staining

To assess neuronal damage, HE staining and Nissl staining (Solarbio, Beijing, China) were performed following the manufacturer's protocols. After staining, sections were examined and imaged using a digital imaging system (OPLENIC, Japan). Neuronal density and morphology were analyzed, and the number of neurons was quantified using ImageJ software.

Immunohistochemistry

Paraffin-embedded hippocampal sections were deparaffinized and rehydrated, followed by immunostaining procedures performed according to the protocols of the DAB and IHC kits (MXB Biotechnology, Fuzhou, China). Primary antibodies used included anti-Syn (1:100, Proteintech, Wuhan, China) and anti-PSD95 (1:100, Proteintech, Wuhan, China). Positive staining signals were visualized under a light microscope, and the immunoreactive area was quantified using ImageJ software.

Cell culture

N2a cells were cultured in DMEM/F12 medium (Gibco, USA) supplemented with 10% fetal bovine serum (FBS, Oricell, USA) and maintained in a humidified incubator at 37 °C with 5% CO₂.

Primary hippocampal neurons were isolated from neonatal C57BL/6 J mice within 24 h after birth. Briefly, hippocampal tissues were dissected in pre-cooled DMEM/F12 medium under sterile conditions and minced into small fragments. The tissue was digested with 0.05% trypsin containing DNase I at 37 °C for 15 min. Digestion was terminated by adding medium containing FBS, followed by centrifugation and filtration through a 0.45-μm cell strainer. The resulting cell pellet was resuspended in complete culture medium. Cells were plated at a density of 3 × 10⁵ cells/mL for immunofluorescence assays and 8 × 10⁵ cells/mL for Western blot analysis. After 3 h of initial attachment, the medium was replaced with

Neurobasal medium (Gibco, USA) supplemented with 2% B27 (Gibco, USA), 1% GlutaMAX, and 1% penicillin–streptomycin (Solarbio, Beijing, China) to support neuronal survival and maturation.

Immunofluorescence staining

At DIV2 and DIV4, neurons cultured on poly-D-lysine-coated coverslips were fixed with 4% paraformaldehyde for 20 min and permeabilized with 0.3% Triton X-100 in PBS for 10 min. After blocking with 5% BSA for 1 h, cells were incubated overnight at 4 °C with anti-MAP2 antibody (1:1000, Abcam, UK). After washing, cells were incubated with Alexa Fluor-conjugated secondary antibody (1:500, Abcam, USA) for 1 h at room temperature in the dark. Coverslips were mounted with antifade mounting medium and imaged using an FV3000 laser scanning confocal microscope (Olympus, Japan). Axonal length was quantified using ImageJ software.

Real-time quantitative polymerase chain reaction (qPCR)

Total RNA was extracted from collected cells using TRIzol Reagent (Invitrogen, CA, USA) according to the manufacturer's instructions. Reverse transcription was performed using the TransScript® First-Strand cDNA synthesis SuperMix (TransGen Biotech, Beijing, China) to synthesize complementary DNA (cDNA). Quantitative PCR was carried out using SYBR Green Master Mix (Roche, Basel, Switzerland) on a real-time PCR system. Gene expression levels were analyzed using the 2^{-ΔΔCt} method, with β-actin as the internal reference gene. Primer sequences are listed in Additional file 1: Table S1.

Western blot

N2a cells were treated with varying concentrations of sodium NaLA, dichloroacetate (DCA), or oxamate for 24 h, or co-treated with 15 mM NaLA and 10 μM Aβ1–42 for 24 h. For primary hippocampal neurons, 5 mM NaLA was added at DIV1, and cells were harvested at DIV2 and DIV4. Western blot was performed as previously described [32]. Following treatment, cells were lysed in RIPA buffer supplemented with protease and phosphatase inhibitors (Beyotime, Shanghai, China), and centrifuged at 12,000 ×g for 15 min at 4 °C. Protein concentrations were determined using a BCA Protein Assay Kit (Beyotime, Shanghai, China). Equal amounts of protein were separated by SDS-PAGE and transferred onto PVDF membranes (Millipore, USA). After blocking with 5% non-fat milk, membranes were incubated overnight at 4 °C with primary antibodies including anti-Syn (1:1000, Proteintech,

Wuhan, China), anti-PSD95 (1:1000, Proteintech, Wuhan, China), and anti- α -Tubulin (1:1000, Proteintech, Wuhan, China). After incubation with HRP-conjugated secondary antibodies, protein bands were visualized using enhanced chemiluminescence (ECL, Thermo Fisher Scientific, USA) and quantified using ImageJ software.

Transcriptome sequencing (RNA-seq)

Total RNA was extracted from hippocampal tissues using TRIzol reagent (Invitrogen, USA). RNA quality was assessed by NanoDrop and Agilent 2100 Bioanalyzer. High-quality RNA ($\text{RIN} \geq 7.0$) was used for library preparation and sequencing, which were performed by Novogene (Beijing, China). Libraries were constructed using the NEBNext® Ultra™ RNA Library Prep Kit and sequenced on an Illumina NovaSeq 6000 platform (150 bp paired-end reads). Clean reads were aligned to the mouse reference genome (GRCm38/mm10) using HISAT2. Gene expression was quantified using featureCounts and normalized as FPKM. Differentially expressed genes (DEGs) were identified with DESeq2 ($|\log_2 \text{FC}| > 0, p < 0.05$). FDR-adjusted p -values were also calculated using the Benjamini–Hochberg method, but were not used as the primary threshold due to the limited number of DEGs under FDR < 0.05 . Gene Ontology (GO) and Kyoto Encyclopedia of Genes and Genomes (KEGG) enrichment analyses were conducted to explore biological functions and pathways associated with DEGs. The full list of DEGs is provided in Additional file 2: Table S2.

Statistical analysis

Statistical analyses were performed using GraphPad Prism 8.0.2 software. Data are presented as mean \pm SEM. Group differences were analyzed using one-way or two-way ANOVA, followed by Tukey's multiple comparisons test. A p -value < 0.05 was considered statistically significant.

Results

Treadmill exercise attenuates cognitive impairment and synaptic loss in SAMP8 mice

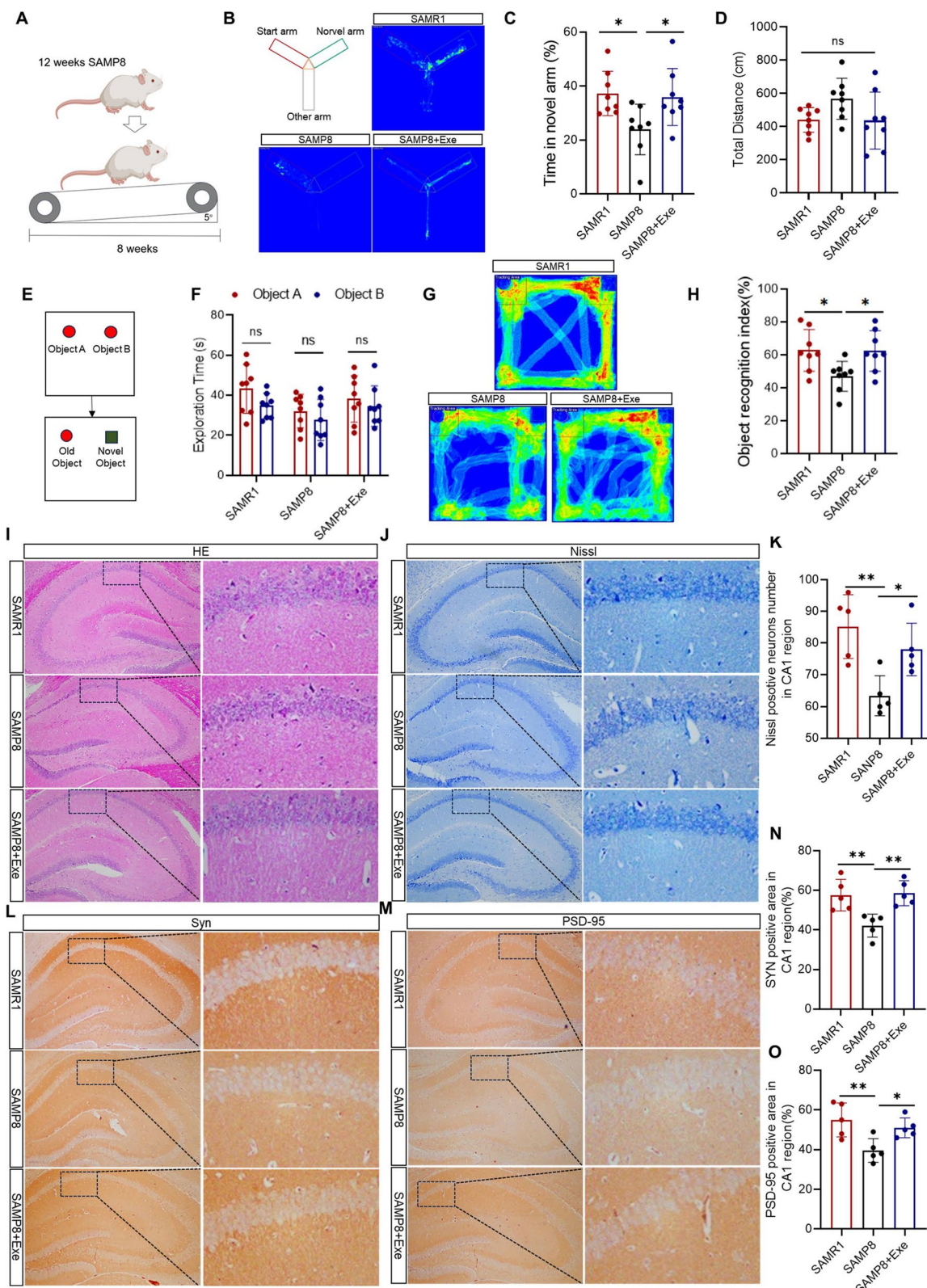
Twelve-week-old SAMP8 mice were subjected to an 8-week treadmill exercise intervention (Fig. 1A). After

the intervention, cognitive function was assessed using the Y-maze test and the NOR test. In the Y-maze, SAMP8 mice exhibited significantly reduced time spent in the novel arm compared to SAMR1 controls, indicating impaired spatial memory. Treadmill exercise significantly increased the time spent in the novel arm in SAMP8 + Exe mice, suggesting a partial rescue of spatial memory deficits (Fig. 1B,C). No significant differences in total distance traveled were observed among groups, excluding locomotor function as a confounding factor (Fig. 1D). In the NOR task, exploration time during the familiarization phase did not differ significantly between the two identical objects in any group, indicating the absence of location bias (Fig. 1E,F). During the testing phase, SAMP8 mice exhibited a lower novel object recognition index than SAMR1 controls, suggestive of impaired recognition memory. Treadmill exercise significantly improved recognition memory in SAMP8 + Exe mice, as evidenced by an increased preference for the novel object (Fig. 1G,H). To assess neuroprotection at the tissue level, we performed HE and Nissl staining in hippocampal sections. Compared to SAMR1 mice, SAMP8 mice exhibited neuronal atrophy, disorganized cellular architecture, and nuclear condensation, indicative of neurodegeneration. However, treadmill exercise markedly alleviated these pathological changes, preserving neuronal morphology and organization (Fig. 1I). Nissl staining further confirmed significant neuronal loss in the CA1 region of SAMP8 mice, which was significantly mitigated by exercise (Fig. 1J,K).

Given that synapses are the structural basis of memory and cognition [33]. Immunostaining was performed to assess the expression levels of synapse-related proteins, including synaptophysin (Syn) and postsynaptic density protein 95 (PSD-95), in the hippocampus. Immunostaining results showed that Syn and PSD-95 expression in the CA1 region of SAMP8 mice was significantly reduced compared to SAMR1 controls (Fig. 1L–O). However, treadmill exercise significantly increased Syn and PSD-95 expression in the SAMP8 + Exe group, indicating a partial reversal of synaptic loss and enhancement of synaptic integrity and plasticity. Together, these findings indicate

(See figure on next page.)

Fig. 1 Treadmill exercise attenuates cognitive impairment and synaptic loss in SAMP8 mice. **A** Experimental design of treadmill exercise intervention in SAMP8 mice. **B** Representative heatmaps of exploration trajectories in the Y-maze test. **C** Quantification of time spent in the novel arm in the Y-maze test ($n = 8$ per group). **D** Total distance traveled in the Y-maze test ($n = 8$ per group). **E** Schematic diagram of the NOR task, including the familiarization phase (two identical objects) and the testing phase (one novel and one familiar object). **F** Exploration time for two identical objects during the familiarization phase ($n = 8$ per group). **G** Representative heatmaps of exploration trajectories in the NOR test. **H** Quantification of new object recognition index in the NOR test ($n = 8$ per group). **I,J** Representative images of hippocampal HE staining and Nissl staining. Left panels: low magnification ($\times 10$); right panels: high magnification ($\times 200$). **K** Quantification of Nissl-positive neurons in the CA1 region ($n = 5$ per group). **L–M** Representative images of Syn and PSD-95 immunohistochemistry. Left panels: low magnification ($\times 10$); right panels: high magnification ($\times 200$). **N,O** Quantification of Syn (L) and PSD-95 (M) expression levels in the CA1 region ($n = 5$ per group). Data are means \pm SEM. * $p < 0.05$, ** $p < 0.01$. Statistical analysis was performed using one-way ANOVA followed by Tukey's multiple comparisons test

**Fig. 1** (See legend on previous page.)

that treadmill exercise mitigates cognitive impairment and synaptic degeneration in SAMP8 mice, potentially through neuroprotection and enhancement of synaptic plasticity.

Treadmill exercise attenuates cognitive impairment and synaptic loss in A β 1–42-induced AD mice

To better model the pathological hallmarks of AD, including A β deposition-induced cognitive decline and synaptic dysfunction, and to explore the beneficial effects of exercise intervention, we established an AD mouse model by bilaterally injecting A β 1–42 into the hippocampus of C57BL/6 J mice, followed by 8 weeks of treadmill training (Fig. 2A). To assess learning and memory performance, the Y-maze test and the MWM test were carried out. In the Y-maze test, the total distance of each mouse showed no significant difference in all groups, A β 1–42 group significantly decreased the duration in the novel arm whereas A β 1–42 + Exe group significantly increased the duration spent in the novel arm compared with the A β 1–42 group (Fig. 2B–D). In the Morris water maze test, A β 1–42 mice exhibited significantly prolonged escape latency compared to Sham controls, indicating deficits in spatial learning ability. This impairment was significantly alleviated by treadmill exercise, as evidenced by a shorter escape latency in the A β 1–42 + Exe group (Fig. 2E). No significant differences were detected in swimming speed and platform crossover numbers on the probe test day (Fig. 2G–H). However, the time spent in the target quadrant was significantly higher in the A β 1–42 + Exe group compared to the A β 1–42 group, indicating an improvement in spatial learning and memory (Fig. 2I). To evaluate the neuroprotective effects of exercise, we performed HE and Nissl staining on hippocampal sections. In the A β 1–42 group, hippocampal neurons were sparsely arranged, with condensed and darkly stained nuclei, indicative of neurodegeneration. These pathological changes were markedly attenuated in A β 1–42 + Exe mice, suggesting a protective effect of exercise (Fig. 2J). Nissl staining further confirmed significant neuronal

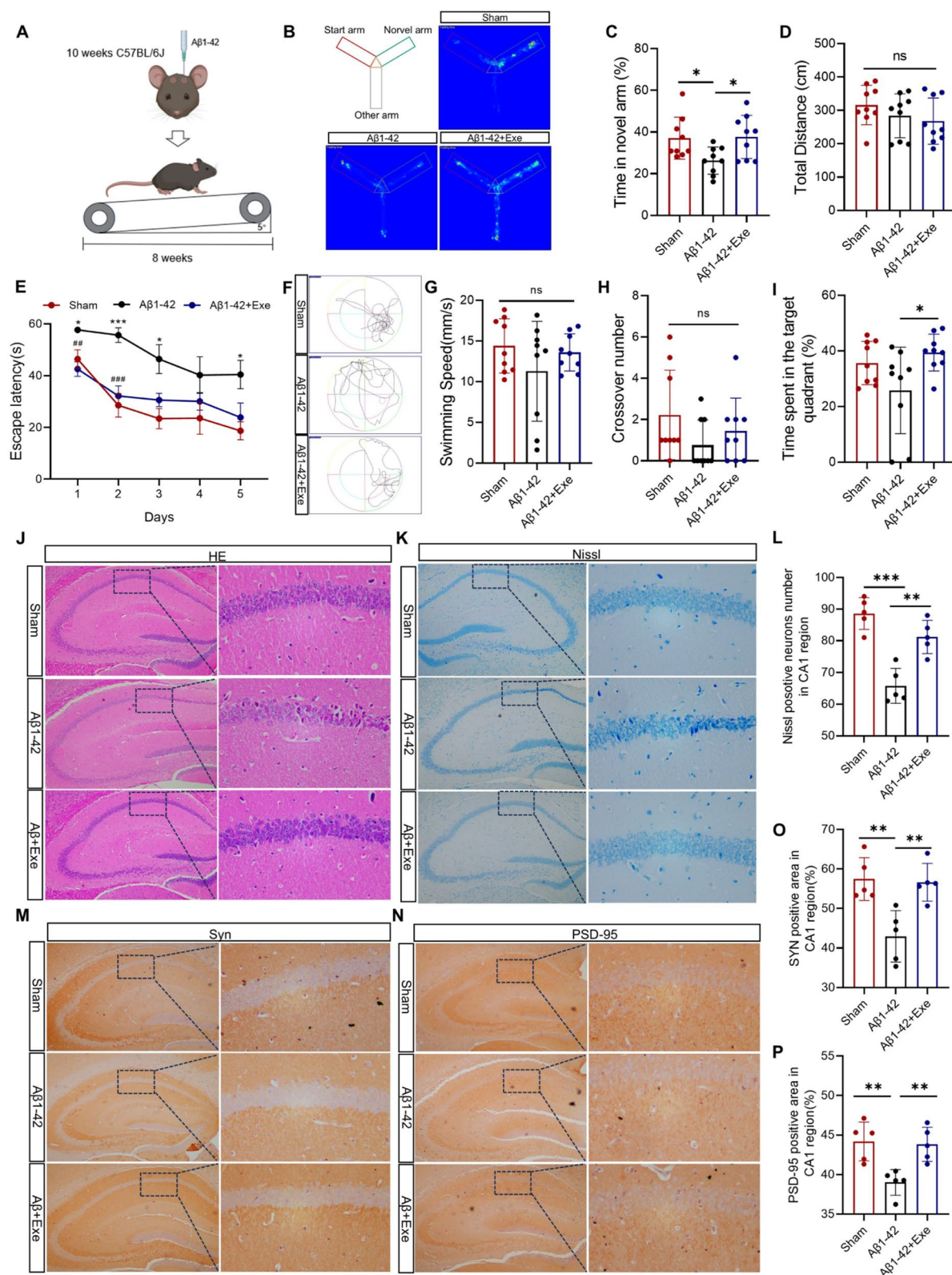
loss in the CA1 region of A β 1–42 mice, which was significantly mitigated by treadmill exercise (Fig. 2K–L). At the synaptic level, immunohistochemical analysis of hippocampal CA1 regions revealed significant reductions in Syn and PSD-95 expression in A β 1–42 mice compared to Sham controls, indicating synaptic loss (Fig. 2M–P). Consistently, Western blot analysis of hippocampal homogenates showed a similar downward trend in the expression of these synaptic markers (Additional file 3: Fig. S1 A). Treadmill exercise significantly increased Syn and PSD-95 expression in the A β 1–42 + Exe group in both assays, demonstrating that exercise promotes synaptic preservation in A β 1–42-induced AD pathology. These results suggest that exercise may improve A β 1–42-induced cognitive dysfunction in mice by ameliorating brain neurodegeneration and synapse loss.

Lactate administration attenuates cognitive impairment in A β 1–42-induced AD mice

Lactate has been reported to play a crucial role in supporting learning, memory, and synaptic plasticity [19, 31, 34]. Following treadmill training, serum lactate levels were significantly elevated in exercised mice compared to sedentary controls (Fig. 3A). To investigate whether exogenous lactate could mimic this effect, we administered sodium NaLA following A β 1–42 injection (Fig. 3B). As expected, NaLA administration significantly increased serum lactate levels compared to the PBS-treated group (Fig. 3C). To evaluate cognitive function, Y-maze and MWM tests were performed. In the Y-maze test, total distance traveled showed no significant differences among groups (Fig. 3E). Compared to the A β 1–42 group, A β 1–42 + NaLA group mice spent significantly more time in the novel arm (Fig. 3F). In the Morris water maze, NaLA administration significantly reduced escape latency compared to the A β 1–42 group, an improvement in spatial memory (Fig. 3G,H). No significant differences were detected in swimming speed or platform crossings during the probe test (Fig. 3J,K). However, the time spent in the target quadrant was significantly increased

(See figure on next page.)

Fig. 2 Treadmill exercise attenuates cognitive impairment and synaptic loss in A β 1–42-induced AD mice. **A** Experimental design of treadmill exercise intervention in A β 1–42-injected mice. **B** Representative heatmaps of exploration trajectories in the Y-maze test. **C** Quantification of time spent in the novel arm in the Y-maze test ($n = 9$ per group). **D** Total distance traveled in the Y-maze test ($n = 9$ per group). **E** Escape latency during training days in the Morris water maze test ($n = 9$ per group). **F** Representative swim trajectories in the probe test of the Morris water maze. **G** Swimming speed during the probe test ($n = 9$ per group). **H** Number of platform crossings during the probe test ($n = 9$ per group). **I** Quantification of time spent in the target quadrant during the probe test ($n = 9$ per group). **J,K** Representative images of hippocampal HE staining and Nissl staining. Left panels: low magnification ($\times 10$); right panels: high magnification ($\times 200$). **L** Quantification of Nissl-positive neurons in the CA1 region. Left panels: low magnification ($\times 10$); right panels: high magnification ($\times 200$). **M,P** Quantification of Syn and PSD-95 expression levels in the CA1 region ($n = 5$ per group). Data are means \pm SEM. * $p < 0.05$, ** $p < 0.01$, *** $p < 0.001$. Statistical analysis was performed using Student's two-tailed *t*-tests (E) or one-way ANOVA, followed by Tukey's multiple comparisons test

**Fig. 2** (See legend on previous page.)

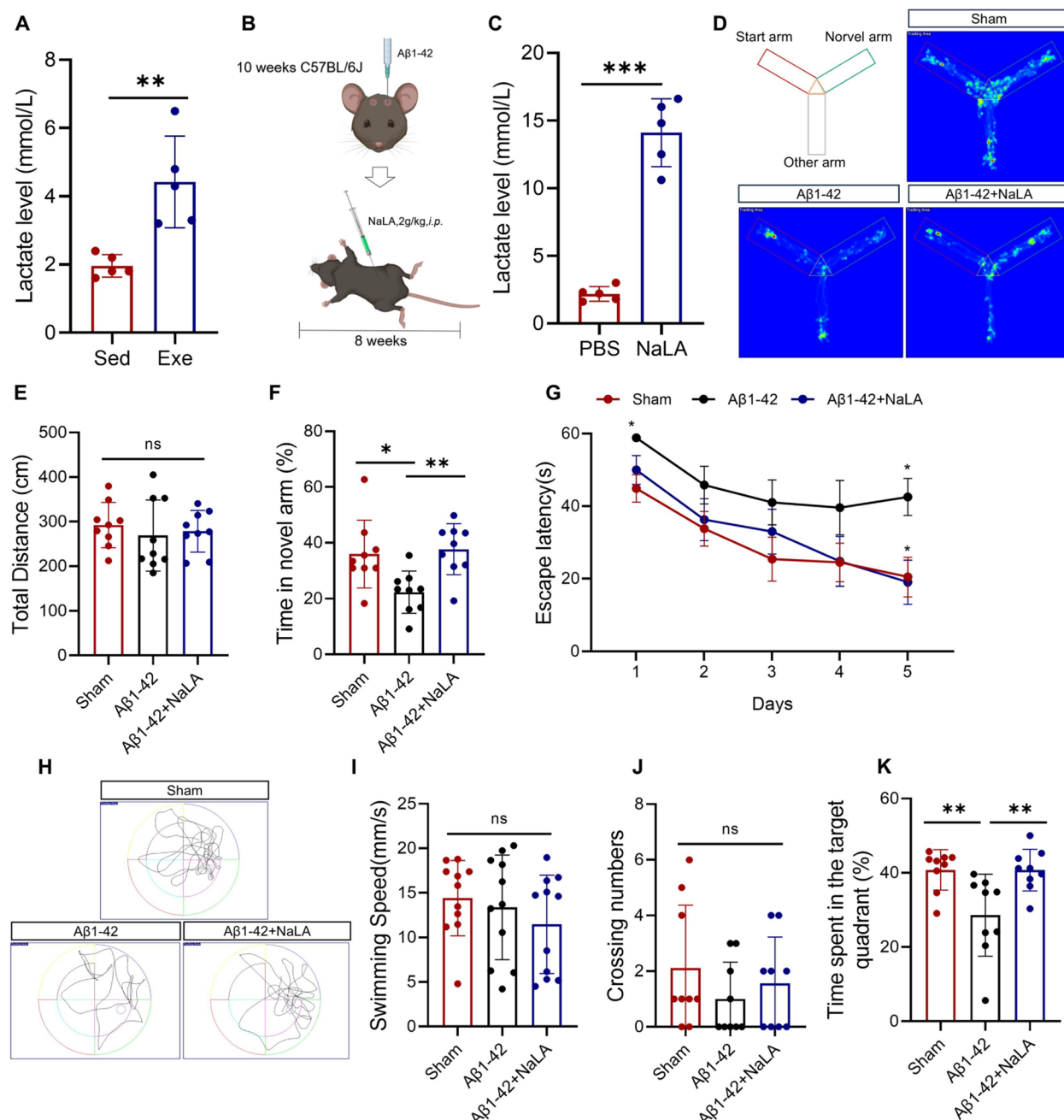


Fig. 3 Lactate administration attenuates cognitive impairment in A β 1-42-induced AD mice. **A** Serum lactate levels in exercised and sedentary mice ($n = 5$ per group). **B** Experimental design of sodium NaLA administration in A β 1-42-injected mice. **C** Serum lactate levels following NaLA treatment ($n = 5$ per group). **D** Representative heatmaps of exploration trajectories in the Y-maze test. **E** Total distance traveled in the Y-maze test ($n = 9$ per group). **F** Quantification of time spent in the novel arm in the Y-maze test ($n = 9$ per group). **G** Escape latency during training days in the Morris water maze test ($n = 9$ per group). **H** Representative swim trajectories in the probe test of the Morris water maze. **I** Swimming speed during the probe test ($n = 9$ per group). **J** Number of platform crossings during the probe test ($n = 9$ per group). **K** Quantification of time spent in the target quadrant during the probe test ($n = 9$ per group). Data are means \pm SEM. * $p < 0.05$, ** $p < 0.01$, *** $p < 0.001$. Statistical analysis was performed using Student's two-tailed t-tests (**G**) or one-way ANOVA, followed by Tukey's multiple comparisons test

in NaLA-treated mice compared to the A β 1-42 group (Fig. 3I). These results suggest that NaLA treatment ameliorates A β 1-42-induced spatial learning and memory impairments.

Lactate modulates synaptic and axonal gene networks in A β 1-42-induced AD mice

To explore the molecular mechanisms underlying lactate-mediated neuroprotection, we performed RNA-seq

analysis on hippocampal tissues from NaLA-treated A β 1–42 mice. A total of 962 DEGs were identified, including 539 upregulated and 423 downregulated genes ($\text{Log}_2 \text{FC} > 0, p < 0.05$) (Fig. 4A). GO enrichment analysis of upregulated DEGs revealed significant involvement in axonogenesis, synapse organization, and dendrite development (Fig. 4B). Cellular component analysis indicated that many DEGs were associated with synaptic structures, including postsynaptic specialization, asymmetric synapse, and postsynaptic membrane (Fig. 4B). KEGG pathway enrichment analysis revealed that DEGs were significantly enriched in pathways such as axon regeneration and axon guidance, suggesting that lactate may facilitate neuronal connectivity and structural plasticity

(Fig. 4C). To further examine the impact of NaLA on genes associated with axonal growth and synaptic organization, we performed heatmap analysis, which revealed significant upregulation of genes involved in these processes (Fig. 4D). Notably, multiple Eph receptor A (Epha) family genes, including Epha4, Epha5, Epha6, and Epha7, were significantly upregulated in the A β 1–42+ NaLA group compared to A β 1–42 mice. EphA receptors have been implicated in synaptic plasticity, axonal guidance, and dendritic spine remodeling [35–38]. To validate these transcriptomic findings, qPCR analysis was performed in NaLA-treated N2a cells, confirming a significant increase in Epha1, Epha2, Epha3, Epha4, Epha5, and Epha7 expression, whereas EphB subfamily members remained

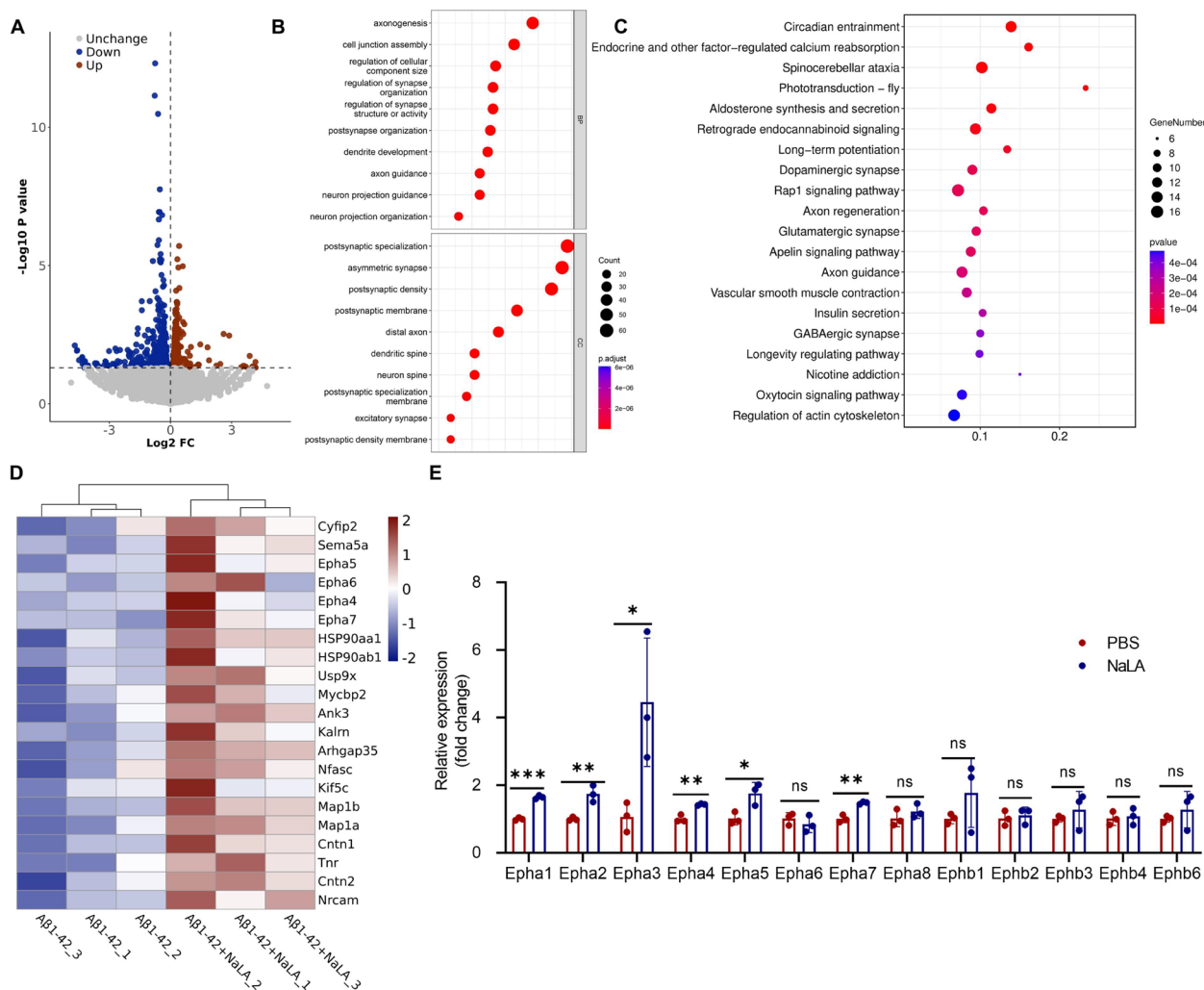


Fig. 4 Lactate modulates synaptic and axonal gene networks in A β 1–42-induced AD mice. **A** Volcano plot of DEGs in the hippocampus between A β 1–42+NaLA and A β 1–42 groups. **B** GO enrichment analysis of upregulated genes, including biological process (BP) and cellular component (CC) terms. **C** KEGG pathway enrichment analysis of upregulated genes. **D** Heatmap showing upregulated genes associated with axon guidance and synaptic organization. **E** qPCR validation of Eph receptor gene expression in NaLA-treated N2a cells ($n=3$ per group). Data are means \pm SEM. Statistical analysis was performed using one-way ANOVA followed by Tukey's multiple comparisons test. * $p < 0.05$, ** $p < 0.01$, *** $p < 0.001$

largely unchanged (Fig. 4E). These results suggest that lactate promotes neuronal resilience by modulating gene networks related to axon guidance and synaptic plasticity, which may contribute to its neuroprotective effects in AD. These results suggest that lactate promotes neuronal resilience and connectivity by modulating axon guidance and synaptic plasticity-related gene networks, potentially contributing to its neuroprotective effects in AD.

Lactate promotes synaptic protein expression and axonal growth

To further validate the impact of NaLA on Synaptic plasticity, we examined Syn and PSD-95 expression in the hippocampal CA1 region using immunohistochemistry. Compared to the A β 1–42 group, NaLA treatment significantly increased Syn- and PSD-95-positive areas, suggesting a reversal of synaptic loss (Fig. 5A–D). In addition, Western blot analysis of hippocampal homogenates further confirmed that NaLA administration elevated Syn and PSD-95 protein levels compared to the A β 1–42 group (Additional file 3: Fig. S1B). In vitro, Western blot analysis of NaLA-treated N2a cells confirmed a dose-dependent increase in PSD-95 and Syn expression (Fig. 5E). Moreover, 15 mM NaLA treatment reversed A β -induced reductions in these synaptic proteins (Fig. 5F). To determine whether endogenous lactate availability regulates synaptic protein expression, we treated cultured N2a cells with Dichloroacetate (DCA, a pyruvate dehydrogenase kinase inhibitor that reduces lactate production) or Oxamate (a lactate dehydrogenase inhibitor that blocks pyruvate-to-lactate conversion). Both inhibitors significantly reduced PSD-95 and Syn expression, reinforcing the role of lactate in synaptic maintenance (Fig. 5G,H). These findings suggest that lactate availability is essential for maintaining synaptic protein stability, exercise-induced lactate elevation contributes to synaptic plasticity.

To further assess the role of NaLA in neuronal morphology, we cultured primary hippocampal neurons with 5 mM NaLA from DIV1. Western blot analysis at DIV2 and DIV4 revealed that NaLA significantly increased PSD-95 and Syn levels compared to the PBS group (Fig. 5I,J). Additionally, to determine whether NaLA promotes neurite outgrowth, axon length was analyzed at DIV2 and DIV4, showing that NaLA-treated neurons exhibited significantly longer axons than PBS-treated controls (Fig. 5K,L).

Lactate transport is required for exercise-induced cognitive and synaptic benefits

Finally, to extend our findings and directly confirm the role of lactate transport in exercise-mediated neuroprotection,

we utilized the 5xFAD transgenic mouse model and administered the lactate transport inhibitor 4-CIN intraperitoneally 1 h prior to treadmill exercise training (Fig. 6A). 4-CIN is a classical inhibitor of MCTs, capable of effectively blocking neuronal lactate uptake without impairing normal neuronal metabolism, and has been confirmed to cross the blood–brain barrier [39, 40]. After the 8-week intervention, cognitive function was evaluated using the Y-maze and MWM tests. In the Y-maze test, treadmill exercise significantly increased time spent in the novel arm compared to sedentary 5xFAD mice, indicating improved spatial memory. However, this beneficial effect was abolished by 4-CIN (Fig. 6B–D). Similarly, treadmill exercise reduced escape latency in the MWM and increased time spent in the target quadrant, effects which were significantly reversed by 4-CIN (Fig. 6E–H). Swimming speed did not differ among groups (Fig. 6I). Furthermore, immunohistochemistry revealed that treadmill exercise reversed the reduction in Syn and PSD-95 expression in the hippocampal CA1 region of 5xFAD mice, an effect attenuated by 4-CIN treatment (Fig. 6J–M). These results indicate that lactate plays an essential role in mediating exercise-induced cognitive enhancement and synaptic protection in AD mice (Fig. 7).

Discussion

In this study, we demonstrate that treadmill exercise improves cognitive function and enhances synaptic plasticity in AD mouse models, with lactate emerging as a critical mediator of these neuroprotective effects. Specifically, treadmill exercise reverses cognitive deficits and synaptic loss in AD mice, improving spatial memory and increasing synapse-associated protein expression. Systemic administration of sodium NaLA mimics the beneficial effects of exercise, supporting a key role for lactate in mediating neuroprotection. Transcriptomic profiling revealed that lactate treatment was associated with modulation of gene networks related to axon guidance and synaptic plasticity, including significant upregulation of several Eph receptor family genes implicated in synaptic remodeling. Blocking lactate transport with 4-CIN abolishes the cognitive and synaptic benefits of exercise, confirming lactate's essential role in exercise-induced neuroprotection. These findings identify lactate as a central effector of exercise-mediated brain resilience and provide a mechanistic basis for targeting lactate metabolism in therapeutic strategies for AD.

Physical exercise is increasingly recognized as a powerful non-pharmacological strategy to mitigate cognitive decline in both aging and neurodegenerative diseases such as AD [41, 42]. While its benefits have been widely reported, few studies have systematically compared its efficacy across multiple AD-related pathologies. To

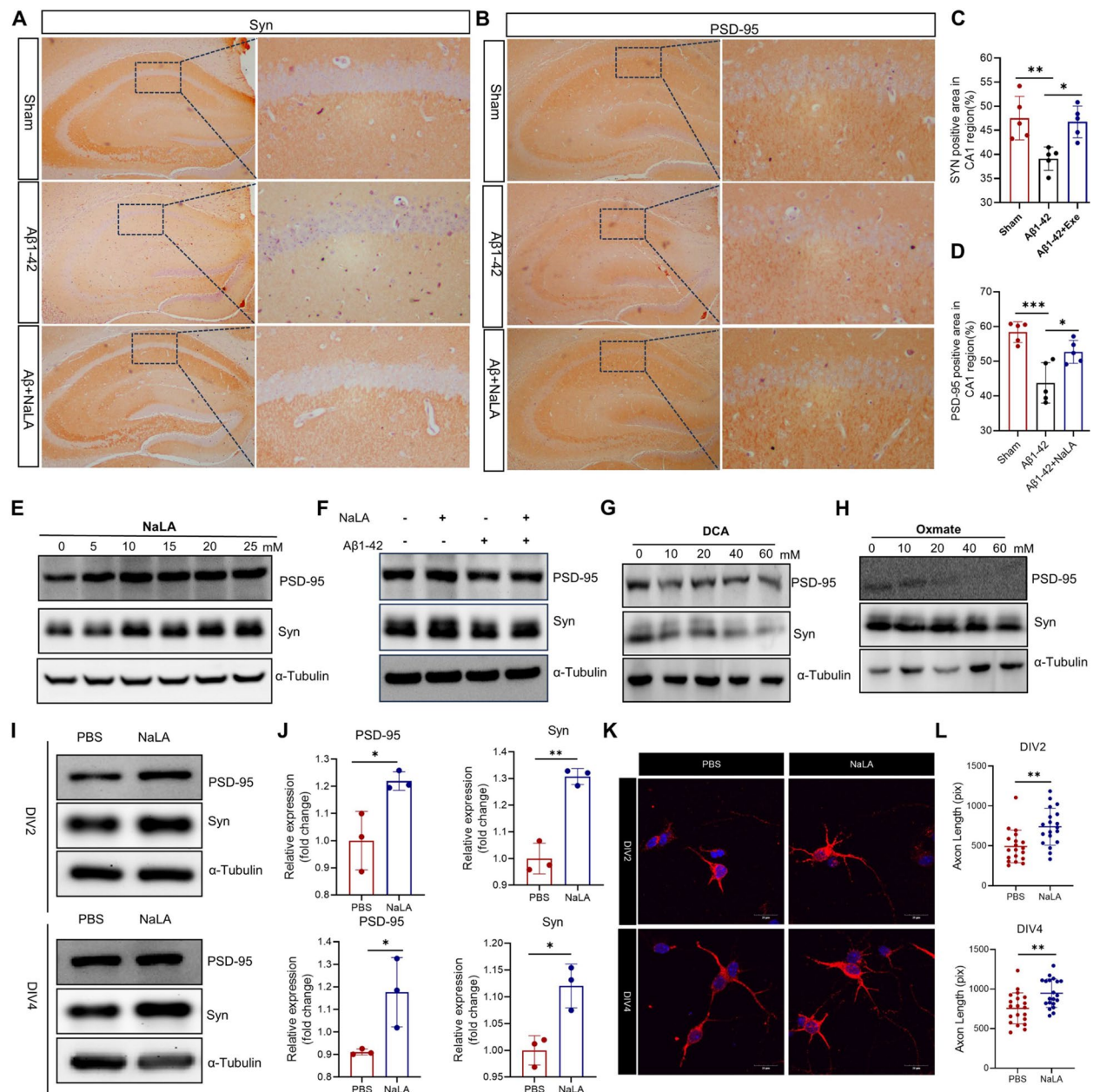


Fig. 5 Lactate promotes synaptic protein expression and axonal growth. **A,B** Representative immunohistochemistry images of Syn and PSD-95 expression in the hippocampal CA1 region. Left panels: low magnification ($\times 10$); right panels: high magnification ($\times 200$). **C,D** Quantification of Syn and PSD-95 expression levels in the CA1 region ($n = 5$ per group). **E** Western blot analysis of PSD-95 and Syn expression in N2a cells treated with increasing concentrations of NaLA. **F** Western blot analysis of PSD-95 and Syn expression following NaLA treatment in A β 1-42-treated N2a cells. **G,H** Western blot analysis of PSD-95 and Syn expression in N2a cells treated with DCA or Oxamate. **I** Western blot analysis of PSD-95 and Syn expression in primary neurons at DIV2 and DIV4, with or without NaLA treatment. **J** Quantification of PSD-95 and Syn expression at DIV2 and DIV4 ($n = 3$ per group). **K** Representative images of immunofluorescence staining showing axon morphology in primary neurons at DIV2 and DIV4. **L** Quantification of axon length at DIV2 and DIV4 ($n = 30$ per group). Data are means \pm SEM. Statistical analysis was performed using one-way ANOVA followed by Tukey's multiple comparisons test. * $p < 0.05$, ** $p < 0.01$, *** $p < 0.001$.

systematically evaluate the generalizability of exercise-induced neuroprotection, we employed three widely used AD-like mouse models: the SAMP8 model, which exhibits age-related cognitive decline; the hippocampal A β 1–42

injection model, mimicking amyloid-induced synaptic toxicity; and the 5xFAD transgenic model, which carries five familial AD mutations and rapidly develops amyloid plaque pathology, neuroinflammation, and cognitive

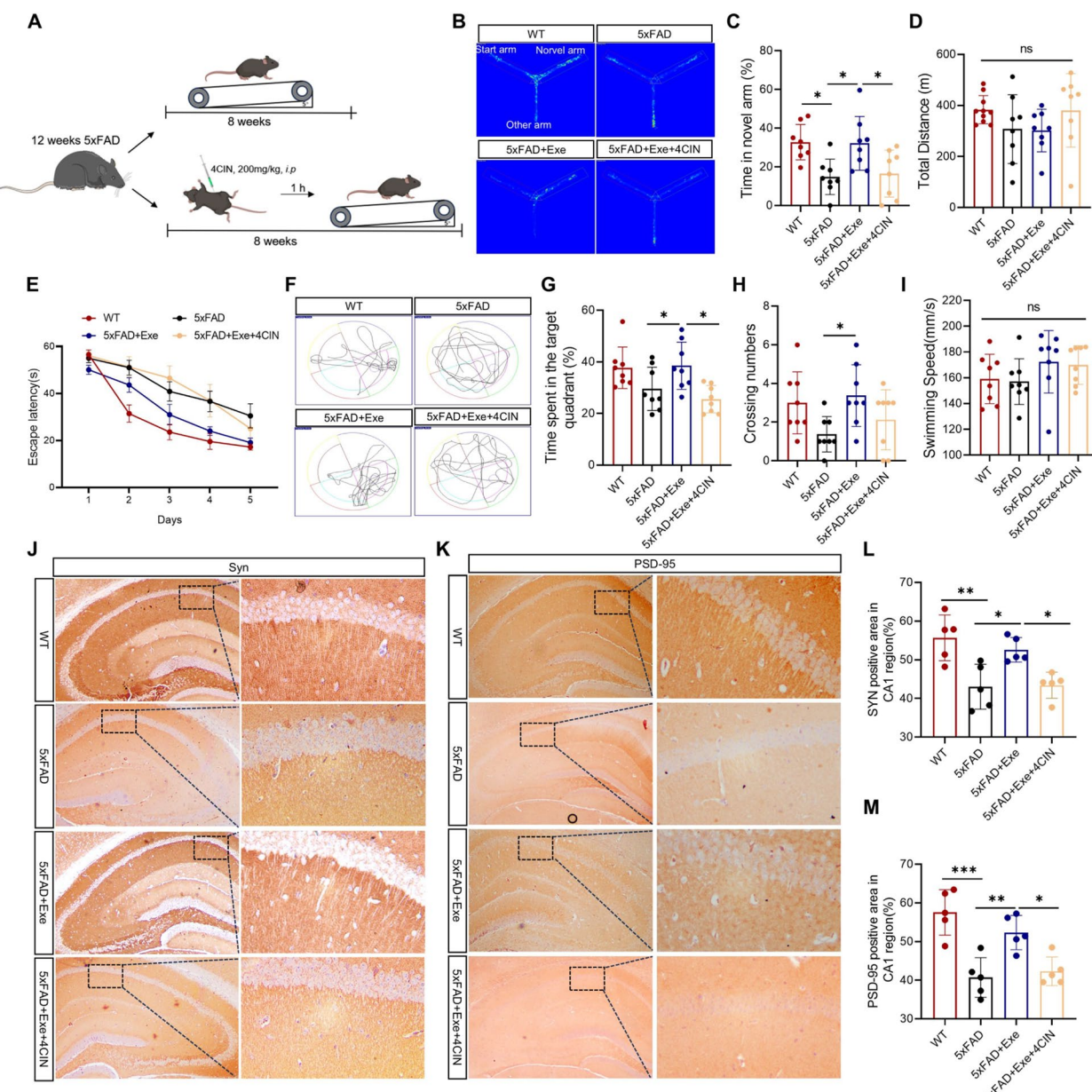


Fig. 6 Lactate transport is required for exercise-induced cognitive and synaptic benefits. **A** Experimental design of treadmill exercise combined with 4-CIN administration in 5xFAD mice. **B** Representative heatmaps of exploration trajectories in the Y-maze test. **C** Quantification of time spent in the novel arm in the Y-maze test ($n = 9$ per group). **D** Total distance traveled in the Y-maze test ($n = 9$ per group). **E** Escape latency during training days in the Morris water maze test ($n = 9$ per group). **F** Representative swim trajectories in the probe test of the Morris water maze. **G** Quantification of time spent in the target quadrant during the probe test ($n = 9$ per group). **H** Number of platform crossings during the probe test ($n = 9$ per group). **I** Swimming speed during the probe test ($n = 9$ per group). **J,K** Representative immunohistochemistry images of Syn (J) and PSD-95 (K) expression in the hippocampal CA1 region. Left panels: low magnification ($\times 10$); right panels: high magnification ($\times 200$). **L,M** Quantification of Syn and PSD-95 expression levels in the CA1 region ($n = 5$ per group). Data are presented as mean \pm SEM. Statistical analysis was performed using Student's two-tailed *t*-tests (E) or one-way ANOVA followed by Tukey's multiple comparisons test. * $p < 0.05$, ** $p < 0.01$, *** $p < 0.001$

impairment. Across all models, treadmill exercise consistently improved cognitive performance, highlighting its robust therapeutic potential in distinct AD-related pathophysiological settings. Given that synaptic dysfunction

is a core pathological feature tightly linked to cognitive decline in AD, it is plausible that the cognitive improvements observed in our study may be attributed [3], at least in part, to enhanced synaptic integrity.

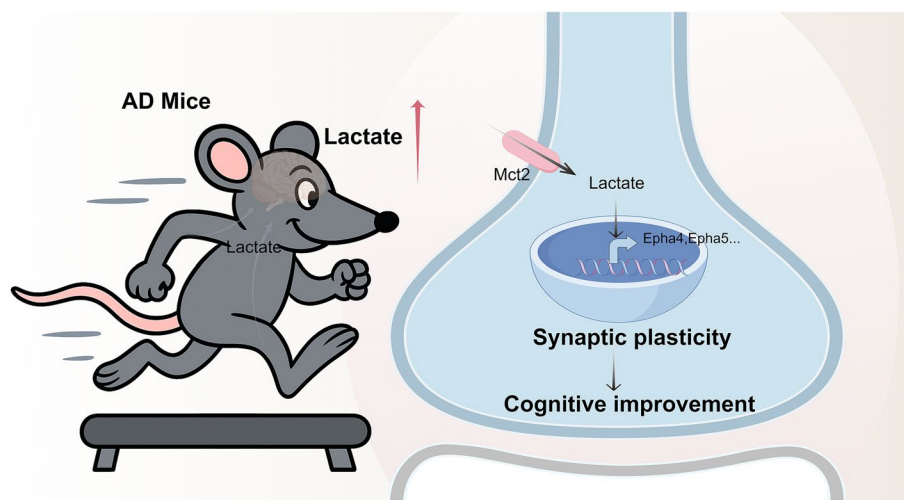


Fig. 7 Schematic overview of the main findings. Treadmill exercise elevates circulating lactate levels, which are subsequently transported into the brain and taken up by neurons via MCT2. Intracellular lactate promotes the expression of synaptic plasticity-related genes, including members of the Eph receptor family (such as EphA4 and EphA5), thereby enhancing synaptic function and ultimately improving cognitive performance

While traditionally considered merely a metabolic byproduct, lactate is now emerging as a critical signaling molecule that connects peripheral metabolic adaptations with central nervous system plasticity [43]. As emphasized by Bergersen, lactate may act as a “volume transmitter” in the brain, exerting its effects through MCTs and associated intracellular pathways [21]. In particular, the neuronal transporter MCT2 is highly localized at postsynaptic membranes of glutamatergic synapses, where it colocalizes with AMPA-type glutamate receptors and PSD-95, suggesting a tight association with activity-dependent synaptic plasticity [44, 45]. Our previous work demonstrated that exercise-induced lactate modulates microglial polarization and alleviates neuroinflammation in AD mouse models [31]. Building upon this, the current study offers multi-level evidence that lactate acts as a key mediator of exercise-induced cognitive and synaptic improvement, extending its relevance beyond immune regulation. We observed a significant elevation in serum lactate levels following treadmill training, suggesting that lactate may function as a critical metabolic effector of exercise-induced neuroprotection. To further validate this hypothesis, we employed a two-pronged experimental approach. First, exogenous administration of NaLA successfully reproduced the cognitive and synaptic benefits observed in exercised mice, indicating that lactate alone is sufficient to drive neuroprotection. Second, pharmacological blockade of lactate transport using 4-CIN in 5xFAD mice abolished the exercise-induced improvements, underscoring the necessity of efficient lactate transport—likely via MCTs—for

mediating these beneficial effects. These findings consolidate the concept that lactate acts not only as a metabolic substrate but also as a key neuromodulator shaping central nervous system function. Moreover, recent findings have expanded the functional landscape of lactate, showing that individual differences in brain lactate levels are associated with effort-based decision-making via modulation of neural activity within the dorsomedial prefrontal cortex (dmPFC) and dorsal anterior cingulate cortex (dACC) [46]. This evidence further underscores lactate’s broad role as a neurometabolic signal linking peripheral metabolic states to central behavioral outcomes.

Consistent with previous reports indicating that lactate enhances hippocampal BDNF expression and activates the SIRT1–PGC1 α –FNDC5 pathway and that lactate receptor HCAR1 activation promotes VEGF-dependent neurogenesis and angiogenesis, our findings further suggest that lactate contributes to exercise-induced brain resilience through a distinct mechanism involving enhanced synaptic protein expression and modulation of gene networks associated with synaptic plasticity and axonogenesis. Our results revealed that lactate-responsive genes were significantly enriched in pathways related to axonogenesis, synapse organization, and dendrite development, suggesting a broader role of lactate in promoting neuronal structural plasticity. Several members of the Eph receptor family were found to be upregulated among these genes; however, whether Eph receptors contribute directly to lactate-mediated neuroprotection requires further investigation [38, 47]. Taken together, our findings provide the first evidence

linking exercise-induced lactate signaling to axonogenesis, establishing a novel mechanistic connection between peripheral metabolic adaptation and structural synaptic remodeling in the context of AD. This extends the functional relevance of lactate beyond traditional neurotrophic pathways, offering new insight into how exercise promotes brain resilience through metabolic-synaptic coupling.

Despite providing compelling evidence, this study has several limitations that warrant consideration. First, although our study employed three widely used AD-like mouse models—SAMP8, A β 1–42 injection, and 5xFAD transgenic mice—to comprehensively evaluate the effects of exercise and lactate, these models only partially recapitulate the complexity of human Alzheimer's disease. Each model reflects distinct pathological features (e.g., aging-related decline or amyloid-driven neurotoxicity), but none fully mimics the multifactorial nature of human AD, which involves tau pathology, vascular dysfunction, and chronic inflammation. Further investigations using integrative or humanized models may better capture disease complexity and facilitate translational applications. Second, transcriptomic analysis revealed significant upregulation of Eph receptor family genes; however, their functional contribution remains to be elucidated. Protein-level validation and mechanistic experiments such as Eph receptor blockade or gene silencing would be valuable for confirming their role in lactate-induced synaptic remodeling. Finally, while transcriptomic analysis revealed significant gene expression changes following NaLA treatment, the underlying regulatory mechanisms remain unclear. We speculate that the neuroprotective effects of lactate may be mediated through multiple complementary mechanisms. Specifically, lactate may serve as an important energy substrate under metabolic impairment conditions such as Alzheimer's disease, rapidly entering neurons via MCTs for oxidative metabolism to support ATP production and mitochondrial functional adaptation [22, 48, 49]. Alternatively, lactate may function as a signaling molecule, activating receptors such as HCAR1 and promoting ERK1/2 phosphorylation, thereby regulating the transcription of genes associated with synaptic plasticity [49, 50]. In addition, lactate-induced histone lactylation may represent a novel epigenetic regulatory mechanism involved in transcriptional modulation [51]. Further studies are needed to elucidate the precise contribution of these mechanisms to lactate-mediated neuroprotection. Finally, all animal experiments were conducted exclusively in male mice, and potential sex-specific differences in the response to exercise and lactate treatment were not evaluated. Moreover, the relatively small sample sizes in some cell-based assays,

such as gene expression analyses, may reduce statistical power. Future studies incorporating both sexes and larger cohorts are warranted to validate and extend the present findings.

Conclusions

This study demonstrates that lactate serves as a critical mediator linking exercise to improvements in cognitive function and synaptic plasticity in Alzheimer's disease models. Treadmill exercise reversed cognitive deficits and synaptic loss, effects that were replicated by systemic administration of sodium NaLA and abolished by 4-CIN-mediated blockade of lactate transport during exercise. Transcriptomic analysis revealed that NaLA modulates gene expression programs related to axon guidance and synaptic remodeling, including upregulation of several Eph receptor family genes. These findings highlight the central role of lactate in exercise-induced neuroprotection and support its potential as a therapeutic target for AD.

Abbreviations

4-CIN	α -Cyano-4-hydroxycinnamic acid
AD	Alzheimer's disease
A β	Amyloid- β
BBB	Blood-brain barrier
BDNF	Brain-derived neurotrophic factor
cDNA	Complementary DNA
dACC	Dorsal anterior cingulate cortex
DCA	Dichloroacetate
DEGs	Differentially expressed genes
dmPFC	Dorsomedial prefrontal cortex
Epha	Eph receptor A
FBS	Fetal bovine serum
GO	Gene Ontology
LTP	Long-term potentiation
MCT	Monocarboxylate transporter
MWM	Morris water maze
NaLA	Sodium L-lactate
NOR	Novel object recognition
PSD-95	Postsynaptic density protein 95
qPCR	Quantitative polymerase chain reaction
RNA-seq	RNA sequencing
Syn	Synaptophysin

Supplementary Information

The online version contains supplementary material available at <https://doi.org/10.1186/s12916-025-04168-x>.

Additional file 1: Table S1. Primer sequences used for qPCR. Forward and reverse primer sequences used in qPCR analysis of Eph receptor genes.

Additional file 2: Table S2. DEGs between A β 1–42+NaLA and A β 1–42 groups identified by transcriptomic profiling. Gene annotation information is included.

Additional file 3: Fig. S1. Western blot analysis of synaptic proteins in the hippocampus of A β 1–42-injected mice.

Additional file 4: Fig. S2. Original Western blot images. Representative uncropped Western blot membranes corresponding to main figures (including PSD-95 and Syn expression in Figure 5 and in Fig. S1).

Acknowledgements

We thank Professor Dan Shao from Sichuan University for her valuable assistance in the construction of animal models. We also gratefully acknowledge all participants and researchers involved in this study for their contributions.

Authors' contributions

HH contributed to performing the experiments, collecting and interpreting the data, and drafting the manuscript. YW contributed to data interpretation, manuscript drafting, and critical revision for important intellectual content. RM, CJ, XY, GW, ZJ, and MZ participated in performing the experiments and data collection. FY, LC, and MZ contributed to critically revising the manuscript for important intellectual content. All authors read and approved the final manuscript.

Funding

This study was supported by the Jilin Province Science and Technology Development Plan Item (No. YDZJ202401253YTS).

Data availability

Data will be made available on request.

Declarations

Ethics approval and consent to participate

All animal procedures were approved by the Ethics Committee of Jilin University [SYXK(JI)2024–0023]. All experiments were conducted in accordance with relevant institutional guidelines and regulations. No human participants were involved in this study.

Consent for publication

Not applicable.

Competing interests

The authors declare no competing interests.

Received: 18 March 2025 Accepted: 27 May 2025

Published online: 03 June 2025

References

1. Zheng Q, Wang X. Alzheimer's disease: Insights into pathology, molecular mechanisms, and therapy. *Protein Cell.* 2025;16(2):83–120.
2. Long JM, Holtzman DM. Alzheimer disease: An update on pathobiology and treatment strategies. *Cell.* 2019;179(2):312–39.
3. Griffiths J, Grant SGN. Synapse pathology in alzheimer's disease. *Semin Cell Dev Biol.* 2023;139:13–23.
4. Shankar GM, Li S, Mehta TH, Garcia-Munoz A, Shepardson NE, Smith I, et al. Amyloid-beta protein dimers isolated directly from alzheimer's brains impair synaptic plasticity and memory. *Nat Med.* 2008;14(8):837–42.
5. Buccellato FR, D'Anca M, Tartaglia GM, Del Fabbro M, Scarpini E, Galimberti D. Treatment of alzheimer's disease: Beyond symptomatic therapies. *Int J Mol Sci.* 2023;24(18):13900.
6. Key MN, Szabo-Reed AN. Impact of diet and exercise interventions on cognition and brain health in older adults: A narrative review. *Nutrients* 2023;15(11):2495.
7. Kivipelto M, Mangialasche F, Ngandu T. Lifestyle interventions to prevent cognitive impairment, dementia and alzheimer disease. *Nat Rev Neurol.* 2018;14(11):653–66.
8. López-Ortiz S, Valenzuela PL, Seisdedos MM, Morales JS, Vega T, Castillo-García A, et al. Exercise interventions in alzheimer's disease: A systematic review and meta-analysis of randomized controlled trials. *Ageing Res Rev.* 2021;72: 101479.
9. Jia RX, Liang JH, Xu Y, Wang YQ. Effects of physical activity and exercise on the cognitive function of patients with alzheimer disease: A meta-analysis. *BMC Geriatr.* 2019;19(1):181.
10. De la Rosa A, Olaso-Gonzalez G, Arc-Chagnaud C, Millan F, Salvador-Pascual A, García-Lucerga C, et al. Physical exercise in the prevention and treatment of alzheimer's disease. *J Sport Health Sci.* 2020;9(5):394–404.
11. Erickson Kl, Voss MW, Prakash RS, Basak C, Szabo A, Chaddock L, et al. Exercise training increases size of hippocampus and improves memory. *Proc Natl Acad Sci U S A.* 2011;108(7):3017–22.
12. Yang L, Wu C, Li Y, Dong Y, Wu CY, Lee RH, et al. Long-term exercise pre-training attenuates alzheimer's disease-related pathology in a transgenic rat model of alzheimer's disease. *Geroscience.* 2022;44(3):1457–77.
13. Wang YY, Zhou YN, Jiang L, Wang S, Zhu L, Zhang SS, et al. Long-term voluntary exercise inhibited age/rage and microglial activation and reduced the loss of dendritic spines in the hippocampi of app/ps1 transgenic mice. *Exp Neurol.* 2023;363: 114371.
14. Mu L, Cai J, Gu B, Yu L, Li C, Liu QS, et al. Treadmill exercise prevents decline in spatial learning and memory in 3xtg-ad mice through enhancement of structural synaptic plasticity of the hippocampus and prefrontal cortex. *Cells.* 2022;11(2):244.
15. Fernandes J, Arida RM, Gomez-Pinilla F. Physical exercise as an epigenetic modulator of brain plasticity and cognition. *Neurosci Biobehav Rev.* 2017;80:443–56.
16. Horowitz AM, Fan X, Bieri G, Smith LK, Sanchez-Diaz Cl, Schroer AB, et al. Blood factors transfer beneficial effects of exercise on neurogenesis and cognition to the aged brain. *Science.* 2020;369(6500):167–73.
17. Ratne N, Jari S, Tadas M, Katariya R, Kale M, Kotagale N, et al. Neurobiological role and therapeutic potential of exercise-induced irisin in alzheimer's disease management. *Ageing Res Rev.* 2025;105: 102687.
18. Wang L, Chen P, Xiao W. B-hydroxybutyrate as an anti-aging metabolite. *Nutrients.* 2021;13(10):3420.
19. Yan L, Wang Y, Hu H, Yang D, Wang W, Luo Z, et al. Physical exercise mediates cortical synaptic protein lactylation to improve stress resilience. *Cell Metab.* 2024;36(9):2104–2117.e2104.
20. Zhao R. Exercise mimetics: A novel strategy to combat neuroinflammation and alzheimer's disease. *J Neuroinflammation.* 2024;21(1):40.
21. Bergersen LH. Lactate transport and signaling in the brain: Potential therapeutic targets and roles in body-brain interaction. *J Cereb Blood Flow Metab.* 2015;35(2):176–85.
22. Park J, Kim J, Mikami T. Exercise-induced lactate release mediates mitochondrial biogenesis in the hippocampus of mice via monocarboxylate transporters. *Front Physiol.* 2021;12: 736905.
23. Brooks GA. The science and translation of lactate shuttle theory. *Cell Metab.* 2018;27(4):757–85.
24. Simpson IA, Carruthers A, Vannucci SJ. Supply and demand in cerebral energy metabolism: The role of nutrient transporters. *J Cereb Blood Flow Metab.* 2007;27(11):1766–91.
25. Suzuki A, Stern SA, Bozdagi O, Huntley GW, Walker RH, Magistretti PJ, et al. Astrocyte-neuron lactate transport is required for long-term memory formation. *Cell.* 2011;144(5):810–23.
26. Qiu LL, Tan XX, Yang JJ, Ji MH, Zhang H, Zhao C, et al. Lactate improves long-term cognitive impairment induced by repeated neonatal sevoflurane exposures through sirt1-mediated regulation of adult hippocampal neurogenesis and synaptic plasticity in male mice. *Mol Neurobiol.* 2023;60(9):5273–91.
27. Fernández-Moncada I, Lavanco G, Fundazuri UB, Bollmohr N, Mountadem S, Dalla Tor T, et al. A lactate-dependent shift of glycolysis mediates synaptic and cognitive processes in male mice. *Nat Commun.* 2024;15(1):6842.
28. Margineanu MB, Mahmood H, Fiumelli H, Magistretti PJ. L-lactate regulates the expression of synaptic plasticity and neuroprotection genes in cortical neurons: A transcriptome analysis. *Front Mol Neurosci.* 2018;11:375.
29. El Hayek L, Khalifeh M, Zibara V, Abi Assaad R, Emmanuel N, Karnib N, et al. Lactate mediates the effects of exercise on learning and memory through sirt1-dependent activation of hippocampal brain-derived neurotrophic factor (bdnf). *J Neurosci.* 2019;39(13):2369–82.
30. Stine WB, Jungbauer L, Yu C, LaDu MJ. Preparing synthetic α β in different aggregation states. *Methods Mol Biol.* 2011;670:13–32.
31. Han H, Zhao Y, Du J, Wang S, Yang X, Li W, et al. Exercise improves cognitive dysfunction and neuroinflammation in mice through histone h3 lactylation in microglia. *Immun Ageing.* 2023;20(1):63.
32. Zhao J, Zhang T, Liang Y, Zou H, Zhang J. Inhibitory activities of 20(r, s)-protopanaxatriol against epidermal growth factor receptor tyrosine kinase. *Food Chem Toxicol.* 2021;155: 112411.
33. Wang H, Hu Y, Tsien JZ. Molecular and systems mechanisms of memory consolidation and storage. *Prog Neurobiol.* 2006;79(3):123–35.
34. Bueschke N, Amaral-Silva L, Hu M, Santin JM. Lactate ions induce synaptic plasticity to enhance output from the central respiratory network. *J Physiol.* 2021;599(24):5485–504.

35. Verma M, Chopra M, Kumar H. Unraveling the potential of ephA4: A breakthrough target and beacon of hope for neurological diseases. *Cell Mol Neurobiol.* 2023;43(7):3375–91.
36. Martínez A, Otal R, Sieber BA, Ibáñez C, Soriano E. Disruption of ephrin-a/epha binding alters synaptogenesis and neural connectivity in the hippocampus. *Neuroscience.* 2005;135(2):451–61.
37. Leonard CE, Baydyuk M, Stepler MA, Burton DA, Donoghue MJ. EphA7 isoforms differentially regulate cortical dendrite development. *PLoS ONE.* 2020;15(12):e0231561.
38. Dines M, Lamprecht R. The role of ephs and ephrins in memory formation. *Int J Neuropsychopharmacol.* 2016;19(4):pyv106.
39. Lev-Vachnish Y, Cadury S, Rotter-Maskowitz A, Feldman N, Roichman A, Illouz T, et al. L-lactate promotes adult hippocampal neurogenesis. *Front Neurosci.* 2019;13:403.
40. Schurr A, Payne RS, Miller JJ, Tseng MT, Rigor BM. Blockade of lactate transport exacerbates delayed neuronal damage in a rat model of cerebral ischemia. *Brain Res.* 2001;895(1–2):268–72.
41. Chen C, Nakagawa S. Physical activity for cognitive health promotion: An overview of the underlying neurobiological mechanisms. *Ageing Res Rev.* 2023;86: 101868.
42. Boa Sorte Silva NC, Barha CK, Erickson KI, Kramer AF, Liu-Ambrose T. Physical exercise, cognition, and brain health in aging. *Trends Neurosci.* 2024;47(6):402–17.
43. Blume GR, Royes LFF. Peripheral to brain and hippocampus crosstalk induced by exercise mediates cognitive and structural hippocampal adaptations. *Life Sci.* 2024;352: 122799.
44. Bergersen LH, Magistretti PJ, Pellerin L. Selective postsynaptic co-localization of mct2 with ampa receptor glur2/3 subunits at excitatory synapses exhibiting ampa receptor trafficking. *Cereb Cortex.* 2005;15(4):361–70.
45. Pierre K, Magistretti PJ, Pellerin L. Mct2 is a major neuronal monocarboxylate transporter in the adult mouse brain. *J Cereb Blood Flow Metab.* 2002;22(5):586–95.
46. Clairis N, Barakat A, Brochard J, Xin L, Sandi C. A neurometabolic mechanism involving dmfc/dacc lactate in physical effort-based decision-making. *Mol Psychiatry.* 2025;30(3):899–913.
47. Lai KO, Ip NY. Synapse development and plasticity: Roles of ephrin/eph receptor signaling. *Curr Opin Neurobiol.* 2009;19(3):275–83.
48. Hu J, Cai M, Shang Q, Li Z, Feng Y, Liu B, et al. Elevated lactate by high-intensity interval training regulates the hippocampal bdnf expression and the mitochondrial quality control system. *Front Physiol.* 2021;12: 629914.
49. Wang MY, Zhou Y, Li WL, Zhu LQ, Liu D. Friend or foe: Lactate in neurodegenerative diseases. *Ageing Res Rev.* 2024;101: 102452.
50. Morland C, Lauritzen KH, Puchades M, Holm-Hansen S, Andersson K, Gjedde A, et al. The lactate receptor, g-protein-coupled receptor 81/hydroxycarboxylic acid receptor 1: Expression and action in brain. *J Neurosci Res.* 2015;93(7):1045–55.
51. Li R, Yang Y, Wang H, Zhang T, Duan F, Wu K, et al. Lactate and lactylation in the brain: Current progress and perspectives. *Cell Mol Neurobiol.* 2023;43(6):2541–55.

Publisher's Note

Springer Nature remains neutral with regard to jurisdictional claims in published maps and institutional affiliations.